

Short Communication

The Effect of Drying and Thickness of TiO₂ Electrodes on the Photovoltaic Performance of Dye-Sensitized Solar Cells

Arman Sedghi, Hoda Nourmohammadi Miankushki*

Imam khomeni International University, Qazvin, 34149-16818, Iran

*E-mail: hoda.nourmohammadi@yahoo.com

Received: 20 September 2014 / *Accepted:* 23 January 2015 / *Published:* 24 February 2015

Dye-sensitized solar cells (DSSC) are based on the absorption of photons by dye, and the transfer of these to TiO₂ electrodes. The microstructure and defects of TiO₂ electrodes are vital for the fabrication of high efficiency dye-sensitized solar cells. These properties strongly relate to the TiO₂ electrode method of fabrication and its parameters. In this research, the effect of drying and thickness of the nanocrystalline TiO₂ electrodes were investigated. Nanocrystalline TiO₂ thin films of different thicknesses were deposited on FTO-coated glass substrates using a tape casting method. Then, these electrodes were dried at different temperatures (130°C and 70°C) at different heating rate. Subsequently, the electrodes were immersed into a dye solution. After dyeing, the cells were assembled using the dye-covered TiO₂ electrodes and platinum-coated FTO and iodine electrolytes. These samples were characterized by SEM, TGA, FTIR, OM and the cell performance then measured by a solar light simulator at an intensity of 1000 W.m⁻². Drying the electrodes at different temperature and different heating rate showed that the solar cells with a TiO₂ electrode dried at 130°C, and at lower heating rate gave a higher short-circuit current density and open circuit voltage, with a higher overall conversion efficiency of 5.1%. The effect of the thickness of TiO₂ films on the parameters of DSSCs was also investigated. Results showed that by increasing the thickness of the TiO₂ films, absorption of the N719 dye through the TiO₂ layers increased to a more optimum level, so that power conversion efficiency (η) of 7.51 % was obtained.

Keywords: dye-sensitized solar cells, titanium dioxide, counter electrode, platinum,

1. INTRODUCTION

The dye-sensitized solar cell (DSSC) is a device for the conversion of visible light into electricity based on the sensitization of wide-band gap semiconductors [1]. The structure of DSSC is consistent with a counter electrode of conductive glass coated with platinum (Pt), a photo anode of TiO₂ porous film on a conductive glass substrate anchored by a monolayer of dye and an electrolyte of

certain organic solvent containing a redox couple such as iodide/tri iodide. When a DSSC is irradiated by sunlight, the electrons of the dye are changed from a ground state to an excited state by absorbing the photons. The excited electrons are injected into the conduction band of TiO₂ porous film and then transferred to the conducting glass through the porous TiO₂ film [2].

The quality, thickness and anchoring of the dye to the surface of TiO₂ are important parameters in determining the efficiency of the cell [3]. Nano-crystalline TiO₂ has been extensively investigated as a potential material for dye-sensitized solar cells [4, 5].

TiO₂ thin films have been prepared via many growth techniques, including tape casting [6], screen printing [7-9], and electro phoretic deposition [10]. Among those methods, the tape casting technique has been more widely employed to prepare nano-TiO₂ coating from pastes [6]. This approach can deposit a porous electrode with high surface area.

In this paper, the preparation of high-quality TiO₂ nanocrystalline thin films on FTO-coated glass substrates by tape casting method and its parameters were investigated. For this purpose, the effects of the drying temperature, heating rate and the film thickness of nanocrystalline TiO₂ films on the photovoltaic performance of DSSC were studied and related to DSSC cell properties.

2. EXPERIMENTAL PROCEDURES

For the fabrication of DSSC devices, TiO₂ paste, N719 dye (both from Dye sol Co.), iodine electrolyte (from Dye sol Co.), H₂PtCl₆ (601450.Merck), TiCl₄ (8.12382.0100.Merck) and deionized water were used. TiCl₄ was diluted with water to 2 M at 0°C to make a stock solution, which was kept in a freezer and freshly diluted to 40 mM for each TiCl₄ treatment of the FTO coated glass plates.

To prepare the DSSC working electrodes, the FTO glasses used as current collector (15Ω/m², Dye sol) were first cleaned in a detergent solution using an ultrasonic bath for 15 minutes, and then rinsed with water and ethanol. After that, the FTO glass plates were immersed into a 40 mM aqueous TiCl₄ solution at 70°C for 30minutes, then washed with water and ethanol. A layer of paste was coated on the FTO glass plates by tape casting, kept in a clean box for 3 minutes in order to homogenize the paste and reduce the surface irregularities, and then dried at 70 °C or 130 °C with different heating rates(medium heating rate (1-2C°/min) and high heating rate(8C°/min)). For increasing thickness these steps were repeated two, three and four times. After drying, the electrodes coated with theTiO₂ pastes were gradually heated under an airflow at 325 °C for 5 minutes, 375 °C for 5 minutes, 450 °C for 15 minutes, and finally, at 500 °C for 15 minutes. The TiO₂ film thus produced were once again treated with 40mM TiCl₄ solution, as described previously, then rinsed with water and ethanol and sintered at 500 °C for 30 minutes. After cooling to 80 °C, the TiO₂ electrodes were immersed into 0.5 mM N-719 dye solution and kept at room temperature for 20–24 hours to assure complete sensitizer uptake.

To prepare the counter electrode, holes were drilled in the FTO glass. The perforated sheet was washed with an H₂O and 0.1 M HCl–ethanol solution and cleaned by ultrasound in an acetone bath for 10 minutes. After removing residual organic contaminants by heating the sheet in air for 15 minutes at 400 °C, the Pt catalyst was deposited on the FTO glasses by dipping the glasses inthe0.2 wt. %H₂PtCl₆

solution and heat-treating it at 400 °C for 15 minutes. The dye-covered TiO₂ electrode and Pt-counter electrode were then assembled into a sandwich-type cell, filled with an electrolyte, and sealed.

A thermal analysis of the TiO₂ paste was accomplished via a differential thermal analysis (DTA [Perkin Elmer Pyris Diamond]) and a thermo gravimetric analysis (TGA [Perkin Elmer Pyris Diamond]) in N₂ atmosphere. This was accomplished by heating the atmosphere 10 °C per minute in order to study evaporation and decomposition reactions during the cell fabrication process. The microstructure and thickness of the TiO₂ film was measured by scanning electron microscopy (SEM) (cam scan MV2300) and optical microscopy (DMI Victory). The TiO₂ paste was characterized by FTIR (Bruker TENSOR 27).

The performance of the dye-sensitized solar cell was examined using a solar simulator at an intensity of 1000 w.cm⁻². The conversion efficiency of the cell was characterized by the short-circuit photocurrent density, the open-circuit voltage, the fill factor of the cell and the intensity of the incident light [11].

$$(1) \quad \eta = J_m V_m / P_{in}$$

$$(2) \quad FF = J_m V_m / J_{sc} V_{oc}$$

In Eq. (1), η is the conversion efficiency of the cell, J_m is the maximum current density, V_m is the maximum voltage, P_{in} the intensity of the incident light, FF is the fill factor, V_{oc} is the open-circuit voltage and J_{sc} is the short-circuit photocurrent density.

3. RESULTS AND DISCUSSION

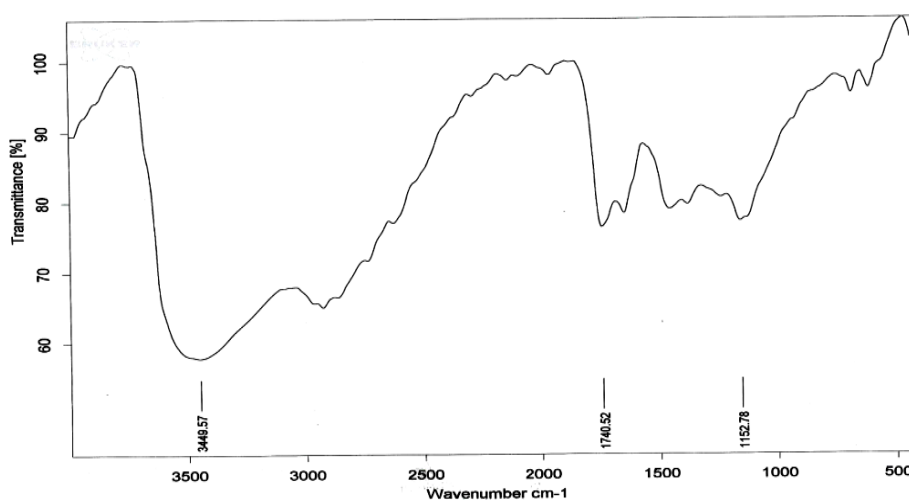


Figure 1. FTIR curve for TiO₂ paste

Figure 1 shows the FTIR curve of the TiO₂ paste (in air with 32 scans per minute). It can be seen that paste had high absorption at about 3449.57 cm⁻¹. This indicated that the amount of alcohol-

based components in the TiO₂ paste was high, so the evaporation of these components had considerable effect on the quality of the TiO₂ film. Alcohol components commence evaporation at low temperatures, so in order to have a defect-free TiO₂ film, evaporation of these components must control precisely.

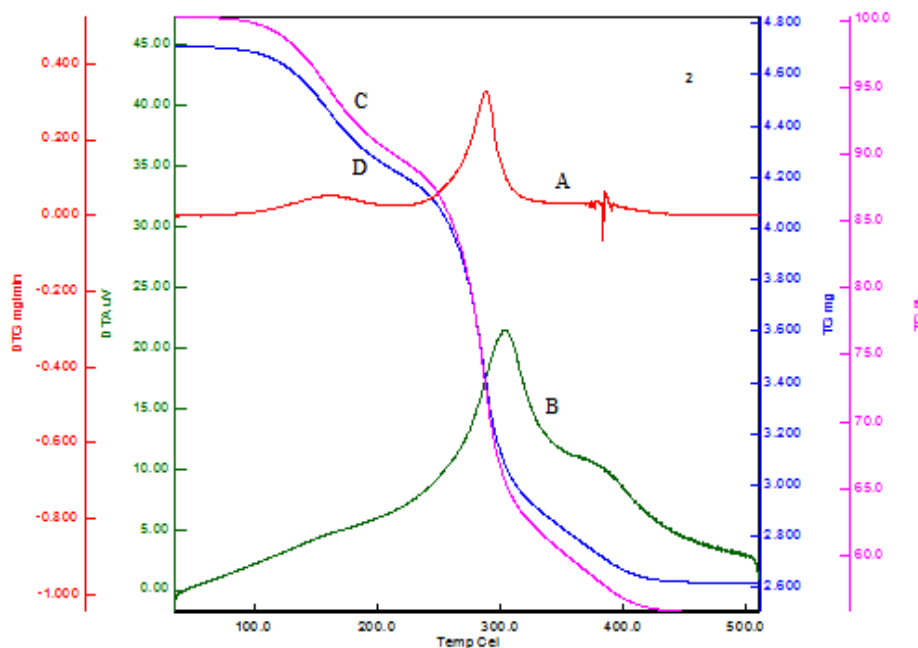


Figure 2. Thermogravimetric analysis (TG: curve C [wt. %] and curve D [weight]) and the corresponding (DTA: curve B and DTG: curve A) for TiO₂ paste

The TGA and DTA of the TiO₂ pastes are shown in Fig. 2. TGA analysis revealed that the paste exhibited an approximate 50% weight loss at temperatures ranging from 100 °C to 300 °C. This is due to the elimination of absorbed water and solvents (mainly alcohols) and the decomposition of organic products. The DTA data indicated that exothermic peaks are associated with the decomposition weight losses at temperatures around 300 °C.

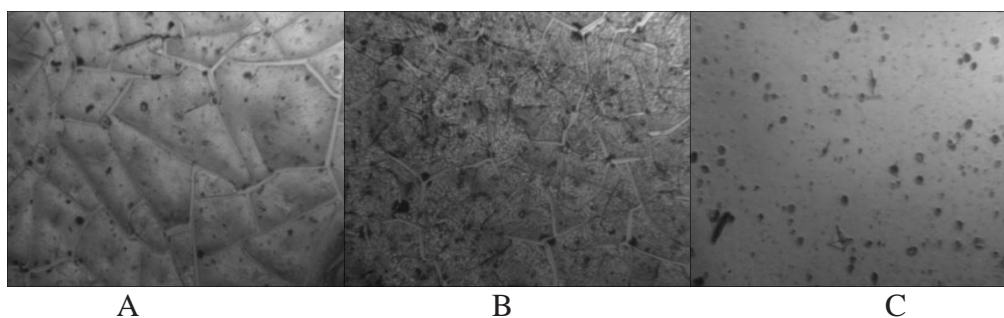


Figure 3. The OM images of TiO₂ film (a) dried at medium heating rate and 70 °C (b) dried at high heating rate and 130 °C; and (c) dried at medium heating rate and 130 °C, 500X

The OM images of different TiO₂ electrodes which dried at different temperatures and different heating rates are shown in Fig.3. According to the TGA analysis, water, solvent and organic products evaporate at temperatures ranging from 100 °C to 150 °C. Drying at low temperatures (up to 70 °C) didn't evaporate these materials from the TiO₂ film, so they evaporated during sintering from the bottom layers and formed surface defects (such as cracks) on the surface of the TiO₂ film. In addition, the heating rate of drying had a strong effect on the amount of film cracks. As the heating rate of the TiO₂ film increased, the paste component exited faster, so the amount of cracks in the TiO₂ film increased.

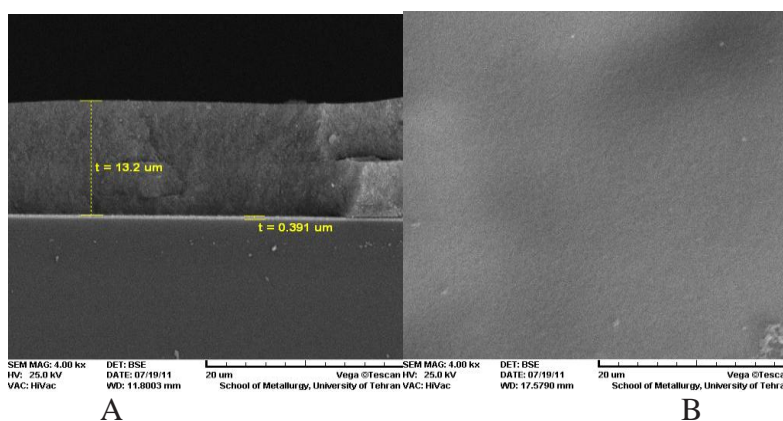


Figure 4. The SEM image of TiO₂ film (dried at 130 °C and medium heating rate) (4.00KX) (a) In cross section (b) from surface

SEM micrographs of the TiO₂ film cross-section (10.3μm), dried at 130 °C via a medium heating rate and annealed at 500°C is shown in Fig. 4. Based on this procedure, no interfacial layer formed between the TiO₂ layer (top) and the FTO layer (bottom). The SEM micrograph also reveals that the film is uniform, smooth and crack-free.

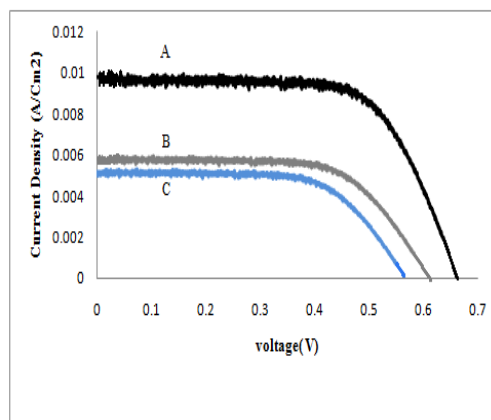


Figure 5. I–V curve for DSSC with different TiO₂ films, A (dried at 130 °C at medium heating rate); B (dried at 130 °C at high heating rate); and C (dried at 70 °C at medium heating rate)

Fig. 5.shows the photocurrent–photo voltage characteristics of the DSSCs with different drying conditions.

Table 1. J–V parameters of cells with different drying rates and temperatures

Number	Temperature (°C)	Heating rate	Short circuit current (Jsc) (mA/cm2)	Open circuit voltage (Voc) (V)	Fill factor	Conversion efficiency (η) (%)
1	70	medium	5.21	0.560	0.74	2.17
2	130	high	6.12	0.585	0.70	2.5
3	130	medium	9.78	0.650	0.78	5.1

Table 1 summarizes the performance data of all devices under the illumination of intensity 100mw/cm2. It can be seen from the table that the photovoltaic characteristics, including the short circuit current density (Jsc), the open circuit voltage (Voc), and the fill factor (FF) and power conversion efficiency are improved when the electrode was dried at 130 °C with a medium heating rate regimen.

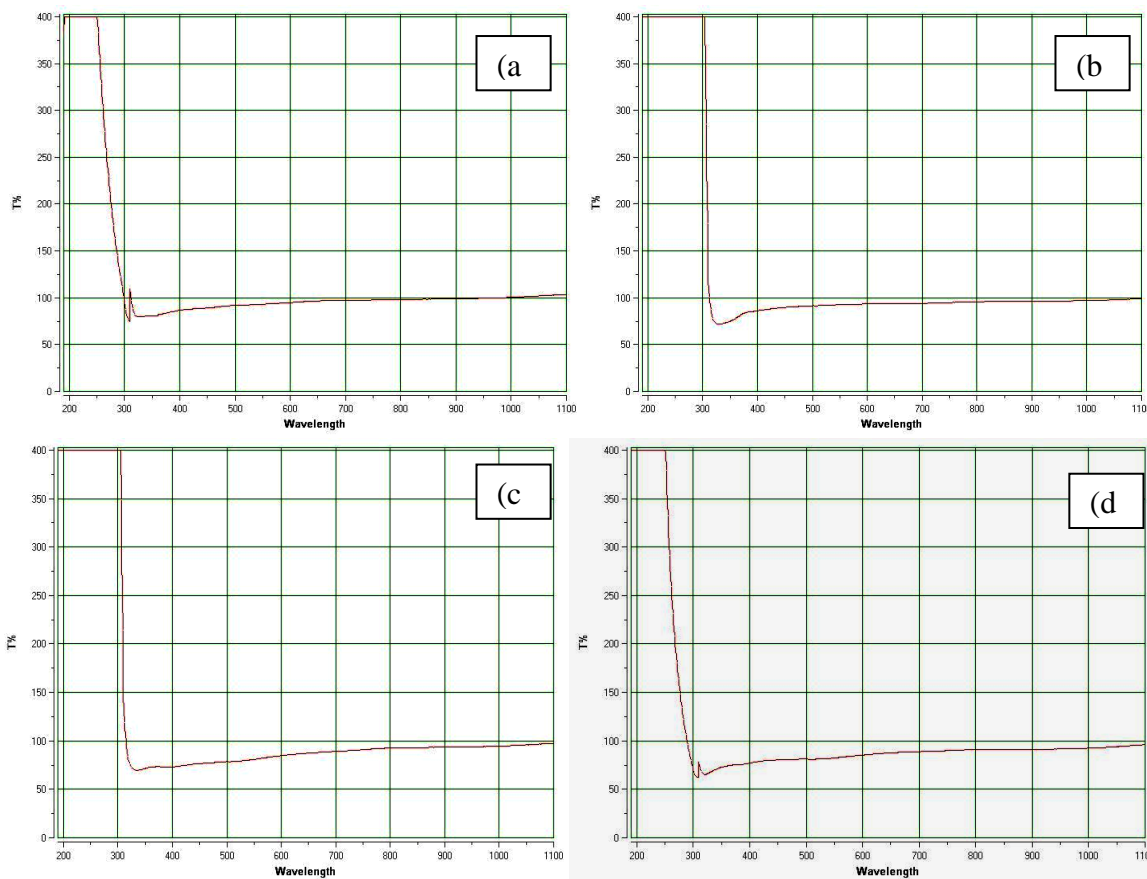


Figure 6. The optical transmittance spectra of TiO2 films with film thicknesses of, (a) 10.3 μm; (b) 13.1 μm; (c) 15.2 μm; and (d) 21.3 μm.

Fig. 6 reveals the UV–visible optical transmittance spectra of the TiO₂ films with different thicknesses between 200 and 1100 nm in wavelength. It can be seen that all films have high transmittance and the absorption edge is at about 300 nm. In addition, the transmittance of the films becomes lower as the films become thicker. The maximum transmittance of the film (a), (b) (c) and (d) in the visible range was about 98%, 95%, 92% and 90%, respectively.

Fig. 7 shows the SEM image of a cross-section of the TiO₂ film with 15.2 μm thickness. The SEM micrograph reveals that the film is uniform, smooth and crack-free.

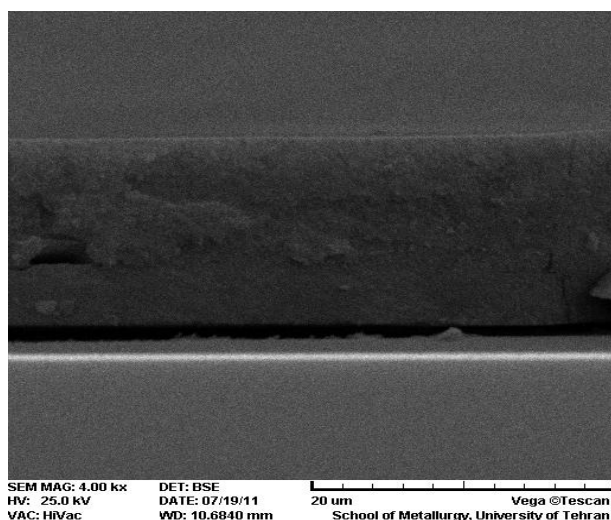


Figure 7. The cross-sectional SEM image of TiO₂ film (15.2 μm)

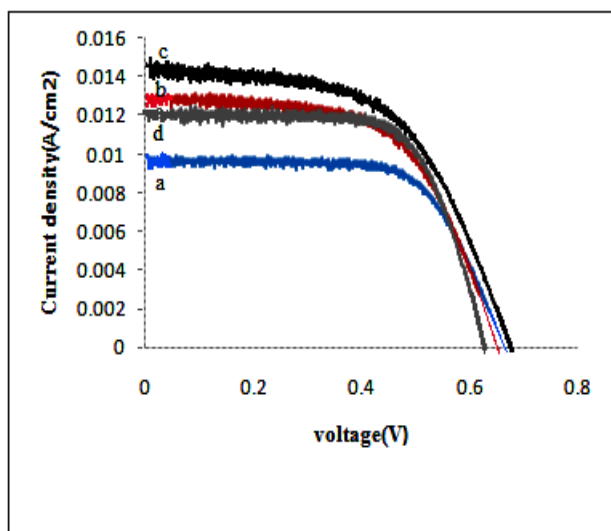


Figure 8. I–V curves for DSSC with different TiO₂ film with film thicknesses of (a) 10.3 μm; 13.1 μm; (c) 15.2 μm; and (d) 21.3 μm.

Fig.8.and Table 2 shows the I–V curves for DSSC with different TiO₂ film thicknesses (10.3–21.3μm) and various fabrication parameters. From these results, the Jsc and Voc of DSSC were

heightened with the increasing of the TiO₂ thin film thickness from 10.3 μm to 15.2 μm. However, the J_{sc} and V_{oc} of DSSC with a TiO₂ film thickness of 21.3 μm (12.1 mA/cm² and 0.631 V) are smaller than those of DSSC with a TiO₂ film thickness of 15.2 μm (14.7 mA/cm² and 0.660 V), respectively. Variations of J_{sc} should be explained by electron photo generation. For a given porosity and pore size, an increase of electrode thickness will directly increase internal surface area and therefore affect dye absorption capabilities. Therefore, a thicker electrode can absorb more photons, which leads to a higher J_{sc}. However, if the electrode thickness is greater than the light penetration depth, the number of photons useful for electron photo generation will reach a limit and, therefore, J_{sc} cannot be further increased. Instead, thickness increase beyond the light penetration depth yields more recombination centers which cause a higher electron loss and thus reduction of J_{sc} [12, 13]. On the other hand, V_{oc} will decrease by increasing electrode thickness.

Table 2. J–V parameters of cells with different thickness

Thickness(μm)	Short circuit current (J _{sc}) (mA/cm ²)	Open circuit voltage (V _{oc}) (V)	Fill factor	Conversion efficiency (η) (%)
10.3	9.78	0.646	0.78	5.1
13.1	12.9	0.641	0.71	5.9
15.2	14.7	0.660	0.77	7.5
21.3	12.1	0.631	0.76	5.7

This phenomenon can be explained by the electron dilution effect [14]. As the light is transmitted into the depth of an electrode, the light intensity gradually decreases [13]. Therefore, as thickness increases, the excessive electron density becomes lower, resulting in a lower V_{oc}. The higher serial resistance of thick electrodes also contributes to the reduction of photo voltage. The decrease in V_{oc} can also be attributed to the increased charge recombination and restricted mass transport in thicker films [15, 16].

4. CONCLUSIONS

1. The effect of the drying temperature and drying rate of the TiO₂ layer on the performance of DSSC showed that the DSSC fabricated with TiO₂ dried at 130 °C with a medium heating rate regimen showed the highest photovoltaic performances. This performance is attributed to the rate of evaporation of water, solvent and organic products, heated at the specified regimen, which reduces electrode defects during sintering.

2. The photovoltaic performance of the DSSC was studied as a function of TiO₂ film thickness. The overall performance of the device will increase as the thickness of TiO₂ layer increases up to a certain thickness. After that point, it slightly decreases. This is attributed to more dye absorption, which leads to more photon absorption, resulting in a higher photocurrent response of the cells. By

increasing the thickness of TiO₂ thin films from 10.3 μm to 15.2 μm, the values of J_{sc} and V_{oc} of DSSC increased from 9.78 to 14.7 mA/cm² and from 0.646 to 0.660 V, respectively. However, the J_{sc} and V_{oc} of DSSC with the 21.1 μm TiO₂ film thicknesses (12.1 mA/cm² and 0.631 V respectively) are smaller than those of with 15.2 μm TiO₂ film thickness (14.7 mA/cm² and 0.660 V respectively). This can be explained by the lower transmittance of too thick TiO₂ thin films (21.1 μm).

3. The corresponding results show that the obtained DSSC with the TiO₂ thin film thickness of 15.2 μm exhibited excellent photovoltaic properties.

References

1. M. Gratzel, *J. Photo chem. Photo biol*, C4 (2003) 145–153.
2. C. Longo and M. De Paoli, *J. Braz. Chem. Soc.*, 14 (6) (2003) 889-901.
3. K. Tennakone, G.R.A. Kumara, A.R. Kumarasinghe, P.M. Sitimanne and K.G.U. Wijayanthe, *J. Photo chem. Photo biol.*, A 94 (1994) 217–220.
4. B. O'Regan and M. Gratzel, *Nature*. 353 (1991) 737–740.
5. A. Hagfeldt, M. Gratzel, *Chem. Rev.* 95 (1995) 49–68.
6. M. K. Nazeeruddin, A. Kay and A. Rodicio, *Jnl. Am. Chem. Soc.*, 115 (1993) 6382.
7. D.S. Tsoukleris and I.M. Arabatzis, *Solar Energy* 79 (2005) 422–430.
8. L. Ma, M. Liu and et al, *Mater. Chem. Phys.* 118 (2009) 477–483.
9. K. Fan, M. Liu, *Renewable Energy* 35 (2010) 555–561.
10. T. Miyasaka, M. Kijitori and et al, *Chem. Lett*, (2002) 1250.
11. Ch. Sh. Chou, Ch. Huang and et al, *Adv. Powder Technol* (2010).
12. M.C. Kao and et al, *Thin Solid Films* 517 (2009) 5096–5099.
13. P. Balraju and et al, *Chemistry* 206 (2009) 53–63.
14. R. Gomez, P. Salvador, *Sol. Energy Mater. Sol. Cells* 88 (2005) 377–388.
15. Z.S. Wang, H. Kawauchi, T. Kashima and H. Arakawa, *Cord. Chem. Rev.* 248 (2004) 1381.
16. S.Y. Huang, G. Schlichthorl, A.J. Nozik, M. Gratzel and A.J. Frank, *J. Phys. Chem. B* 101 (1997) 2576–2582.